On the Power Handling Capability of High Temperature Superconductive Filters

Raafat R. Mansour, *Senior Member, IEEE*, Bill Jolley, Shen Ye, *Member, IEEE*, Fraser S. Thomson, *Member, IEEE*, and Van Dokas

***Abstract*—This paper presents high power test results for high temperature superconductor (HTS) filters having six different configurations. The results demonstrate the possibility of realizing narrow band HTS filters that are capable of handling 30–50 W at 77 K. The paper also introduces a procedure for comparing the power handling capability of HTS filters with different RF characteristics. Issues related to thermal design of high power HTS filters are discussed in detail.**

I. Introduction

THE POWER handling capability of high temperature superconductor (HTS) filters is governed by the quality of the HTS materials as well as the filter geometry and its electrical characteristics. Over the past three years, there has been a strong interest among researchers in the field to develop the HTS materials and filter structures which allow the realization of high power HTS filters [1]–[11]. Several papers have been published on HTS resonators and filters capable of handling modest power levels (few milliwatts) at 77 K. Experimental results have been also reported for wide-band low-order HTS filters capable of handling higher power levels at extremely low temperatures (10–50 K). The lack of a standard procedure to explain the large variations in the published results on power handling capability of HTS filters makes it difficult to assess the true state-of-the-art in high power HTS technology.

There are many parameters which affect the power handling capability of HTS filters. These include: filter bandwidth, filter order, filter unloaded Q, and operating temperature. We present in this paper theoretical and experimental results to illustrate the effect of the above parameters on the power handling capability of HTS filters. Examples are included to demonstrate how one can use these results to compare the power handling capabilities of different HTS filters.

We also present in this paper high power test results for HTS thin film and hybrid dielectric resonator (DR)/HTS filters. The experimental results presented for hybrid DR/HTS filters demonstrate the capability of this type of filter to handle extremely high power levels (30–50 W) at 77 K. Typically, the current density on the resonator elements increases with the reduction of the filter bandwidth and with the increase of filter order. Nevertheless, a remarkable power handling capability has been demonstrated by the 8-pole 1% bandwidth HTS filter considered in this paper.

The problem of temperature rise inside HTS filters is addressed. The measured results presented indicate that a high power HTS filter may switch from a low thermal load to a considerably high thermal load as the HTS materials switch from the superconductive state to the nonsuperconductive state. The paper also presents theoretical results for the electromagnetic field distribution and temperature variation inside HTS filters. The software CAD tools described in this paper can be employed to optimize the thermal design of high power HTS filters.

II. Comparison Between Power Handling Capabilities of Different Filter Structures

Table I illustrates a comparison between the power handling capability of HTS filters having six different filter configurations:

1) 4-pole hybrid DR/HTS filter [12] with 1% bandwidth [YBCO, TBCCO films, Fig. 1(a)];
2) 8-pole hybrid DR/HTS filter [12] with 1% bandwidth [TBCCO films, Fig. 1(b)];
3) 4-pole dual-mode patch resonator filter [13] with 2% bandwidth [TBCCO films, Fig. 1(c)];
4) 3-pole single-mode HTS thin film filter [13] with 4% bandwidth [TBCCO films—50 Ohm impedance, Fig. 1(d)];
5) 3-pole single-mode HTS thin film filter with 1% bandwidth [TBCCO films—12 Ohm impedance, Fig. 1(e)];
6) 6-pole lumped-element HTS thin film filter [14] with 2% bandwidth [TBCCO films, Fig. 1(f)].

The results achieved indicate the importance of the structure geometry and its impact on the power handling capability of HTS filters. The results also show that unpatterned YBCO films can handle as much power as unpatterned TBCCO films at 77 K. The quality of the HTS materials is also a key factor in

Manuscript received October 25, 1995; revised February 12, 1996. This work was supported in part by the Canadian Space Agency (CSA), the Canadian Department of National Defence (DND), and the US Advanced Research Program Agency (ARPA) under the Technology Reinvestment Program, NASA Cooperative agreement NCC 3-344.

The authors are with the Corporate R&D Department, Com Dev Ltd., Cambridge, Ont., Canada.

Publisher Item Identifier S 0018-9480(96)04806-5.

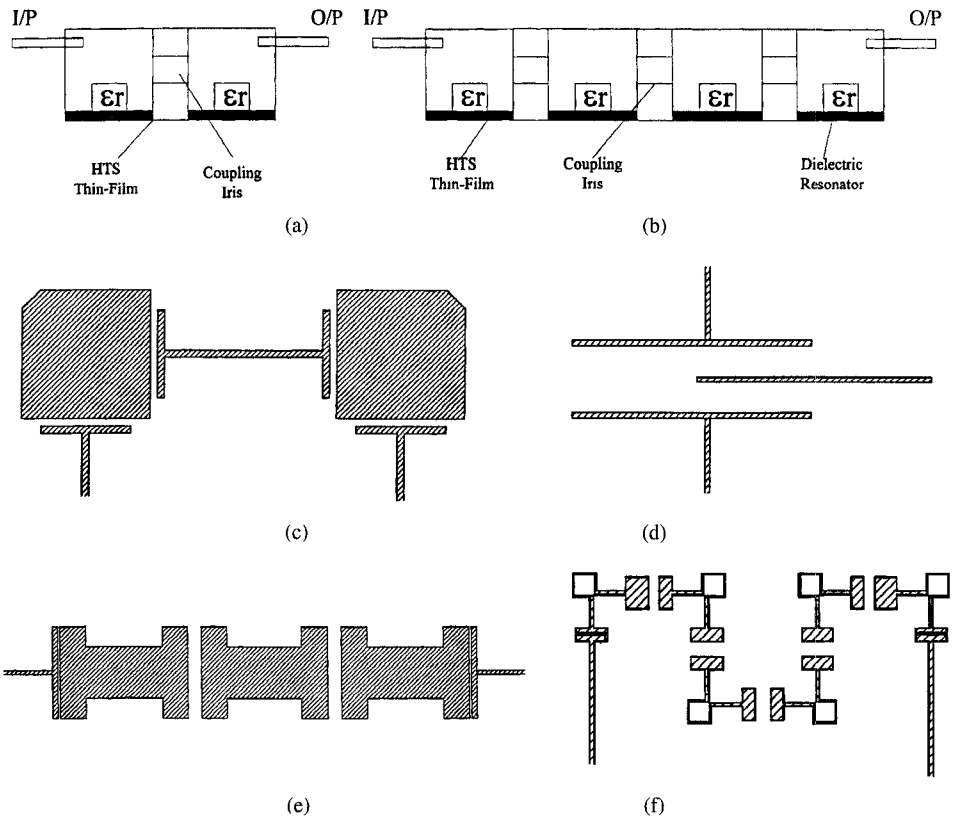

Fig. 1. Layouts of HTS filters tested for high power, filters are identified in Table I.

TABLE I
MAXIMUM POWER OF HTS FILTERS HAVING DIFFERENT CONFIGURATIONS

Filter Structure	Maximum Power * (Testing in Liquid Nitrogen)
4-pole hybrid DR/HTS filter (YBCO films, Figure 1a)	50 watts
4-pole hybrid DR/HTS filter (TBCCO films, Figure 1a)	50 watts
8-pole hybrid DR/HTS filter (TBCCO films, Figure 1b)	30 watts
4-pole patch resonator thin film filter (TBCCO films, Figure 1c)	6 watts
3-pole single-mode thin film filter (TBCCO films, Figure 1d) 50 Ohm impedance	0.7 watts
3-pole single-mode thin film filter (TBCCO films, Figure 1e) 12 Ohm impedance	2.5 watts
6-pole lumped element thin film filter (TBCCO films, Figure 1f)	0.12 watts

+ The maximum power is defined as the power level at which the unloaded Q of the filter degrades by an order of magnitude from the value achievable at an input power of 0 dBm.

designing high power HTS filters. The filter structures given in Table I were built using HTS films supplied by DuPont. These filters have been repeatedly tested for high power using samples from different wafers. The values given in Table I for the maximum power represent the power levels which have been consistently achieved. A dry-etching technique has been used to fabricate the thin film filters shown in Fig. 1(c)–(e).

The insertion loss performance of the four-pole hybrid DR/HTS filter for input power of 10, 20, and 50 W is illustrated in Fig. 2. A small degradation in the insertion loss is observed as the power is increased from 10–50 W. The high

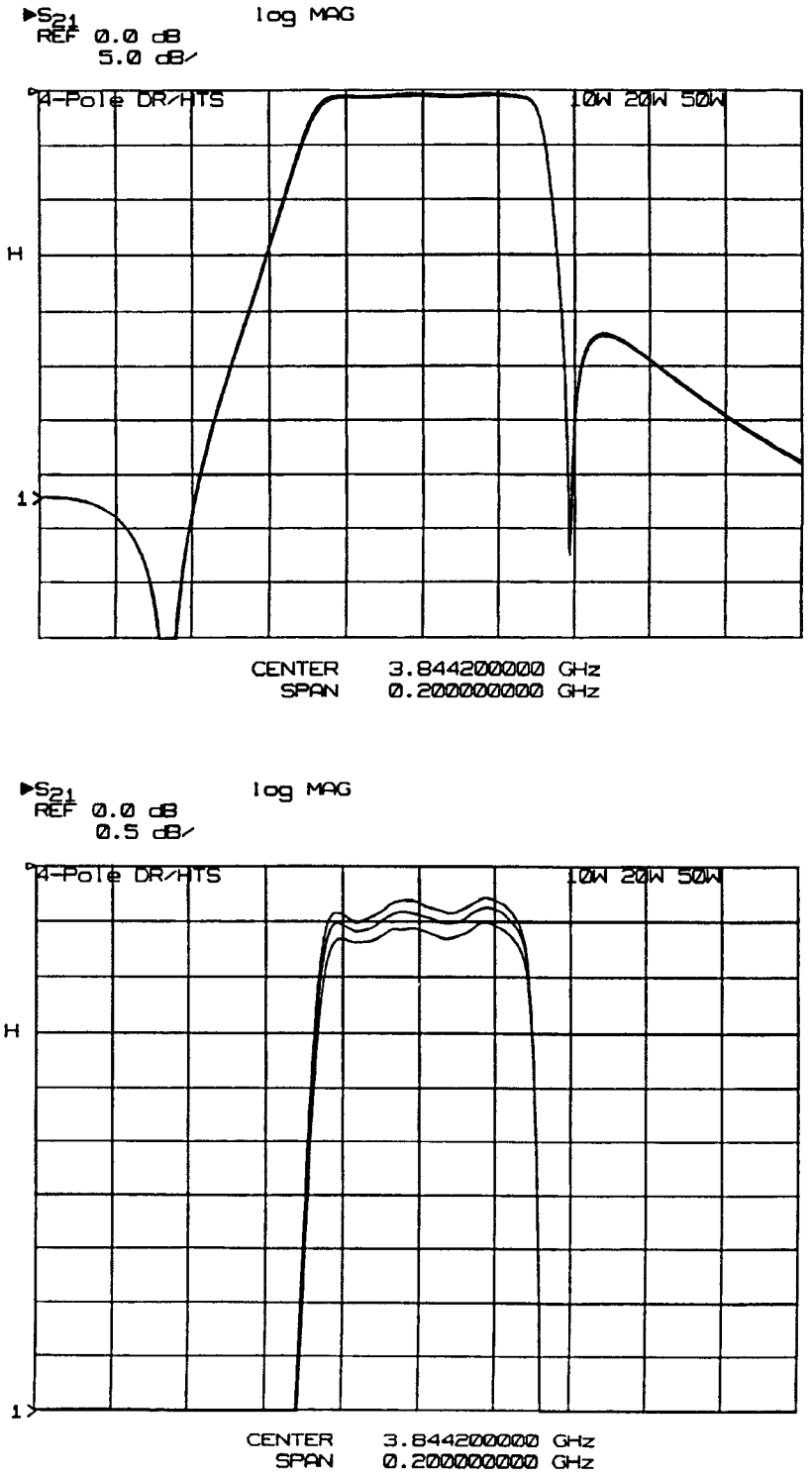

Fig. 2. The insertion loss versus frequency of a four-pole hybrid DR/HTS filter measured under an input power of 10, 20, and 50 W (using a liquid nitrogen dewar).

power test results achieved for the 8-pole hybrid DR/HTS filter and the three-pole thin film filter are shown in Figs. 3 and 4, respectively.

III. Parameters That Affect Power Handling Capability of HTS Filters

The degradation in the superconductor performance is caused by the increased current density in the films as the power level is increased. The current-carrying capability of an individual resonator is determined by the resonator configuration and HTS film characteristics such as film thickness and grain boundaries [5]. However, the amount of current carried by the resonator elements of an HTS filter is mainly governed by filter RF characteristics such as filter order, percentage bandwidth and filter Q. Fig. 5 shows an equivalent circuit of an n-pole filter. The currents flowing on

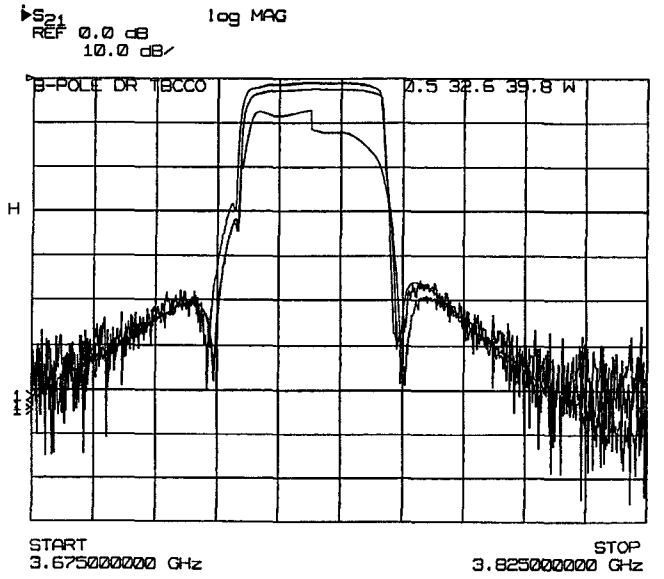

Fig. 3. The insertion loss versus frequency of an 8-pole hybrid DR/HTS filter measured under an input power of 0.5, 32.6, and 39.8 W (using a liquid nitrogen dewar).

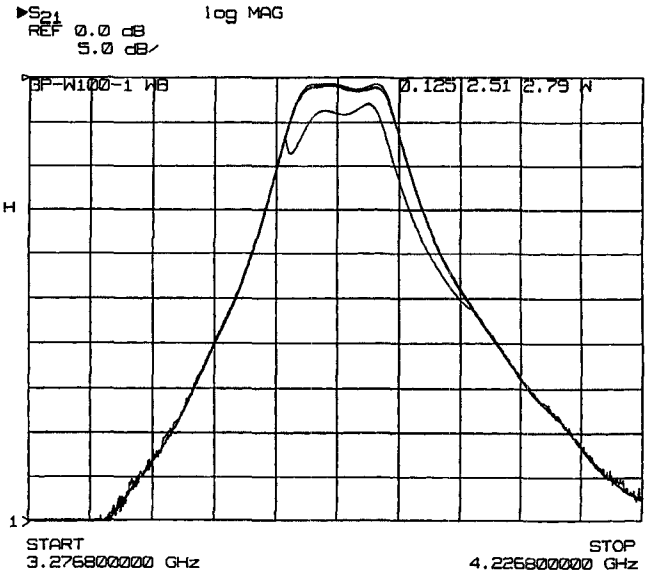

Fig. 4. The insertion loss versus frequency of a three-pole HTS thin filter measured under an input power of 0.125, 2.51, and 2.79 W (using a liquid nitrogen dewar).

the n resonators are given by

$$\begin{bmatrix} i_1 \\ i_2 \\ \vdots \\ i_n \end{bmatrix} = \begin{bmatrix} j\lambda + R_1 + r & j\omega M_{12} & \cdots & j\omega M_{1n} \\ j\omega M_{12} & j\lambda + r & \cdots & j\omega M_{2n} \\ \vdots & & \vdots & \\ j\omega M_{1n} & j\omega M_{2n} & \cdots & j\lambda + r_n + r \end{bmatrix} * \begin{bmatrix} e_1 \\ 0 \\ \vdots \\ 0 \end{bmatrix} \tag{1}$$

where $r = wL/Q$ represents the loss due to the finite Q of the resonator elements. R_1 and R_n are the impedances of the source and load of the circuit and λ represents the resonator impedance. The coupling elements $M_{ij} i = 1 \cdots n$, $j = 1 \cdots n$, are calculated for Chebyshev or elliptic filters using the analysis given in [15]. The input voltage e_1 is determined by the input power level.

A comparison between the simulated current of two four-pole filters designed with a percentage bandwidth of 1 and 4% is given in Fig. 6. It can be seen that in the case of four-pole filters, the HTS resonator #2 would be the first to lose its superconductive characteristics under high power operation. Similar results have been reported in [16] and more recently in [8]. It is also noted that the current flowing on the resonator elements increases with the reduction of bandwidth. In view of the maximum current values shown in Fig. 6(a) and (b), it can be readily shown that a four-pole HTS filter designed with 4% bandwidth should be able to handle close to four times (3.85) more power than an identical filter designed with a 1% bandwidth.

Fig. 7 depicts the simulated current flowing on all eight resonators of an 8-pole filter designed with 1% bandwidth. In view of Figs. 7 and 6(a), it is evident that low-order HTS filters are expected to handle more RF power than high-order filters designed with the same percentage bandwidth. The unloaded Q of the resonators also plays an important role in limiting the power handling capability of the filter. Fig. 8 illustrates the current flowing on a four-pole 0.5% bandwidth filter simulated with unloaded Q values of 2,000 and 10 000. As the unloaded Q increases, more energy will be stored inside the resonator leading to less power handling capability.

IV. A Standard Procedure for Assessing the Power Handling Capability of HTS Filters

The objective of this section is to introduce a standard procedure to compare the power handling capability of different HTS filters. In order to demonstrate this procedure let us consider the following four hypothetical HTS filter structures given below as an example:

1) Structure #1: A three-pole filter, 4% bandwidth, Q = 10,000, measured max. power 95 W;
2) Structure #2: A four-pole filter, 1% bandwidth, Q = 10,000, measured max. power 50 W;
3) Structure #3: A 8-pole filter, 1% bandwidth, Q = 10,000, measured max. power 30 W;
4) Structure #4: A 5-pole filter, 3% bandwidth, Q = 20,000, measured max. power 70 W.

In view of the discussions given in Section III, it is clear that the maximum power level that an HTS filter seems to handle does not necessarily reflect the true power handling capability of the filter structure. An accurate evaluation of the relative performance of the above filters can be achieved by relating the power handling capability of these filters to that of a specific "reference filter," i.e., to estimate the power handling capability that the reference filter would have if it was built

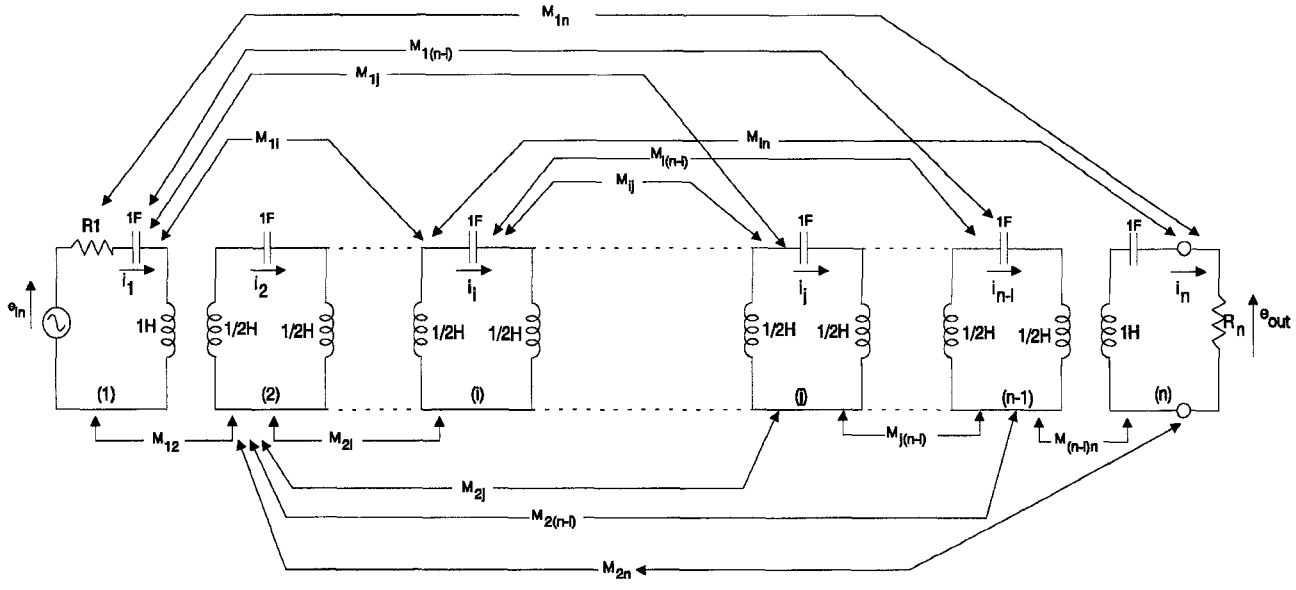

Fig. 5. The equivalent circuit of a generalized n-pole filter.

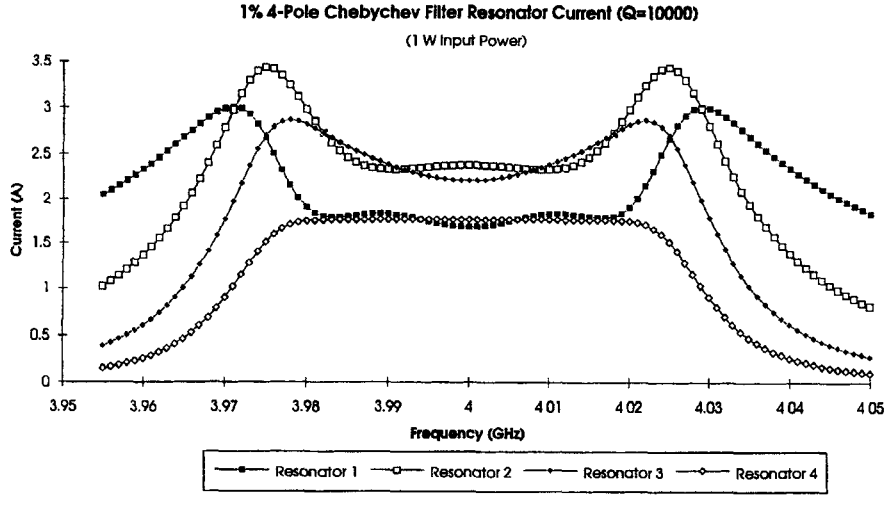

(a)

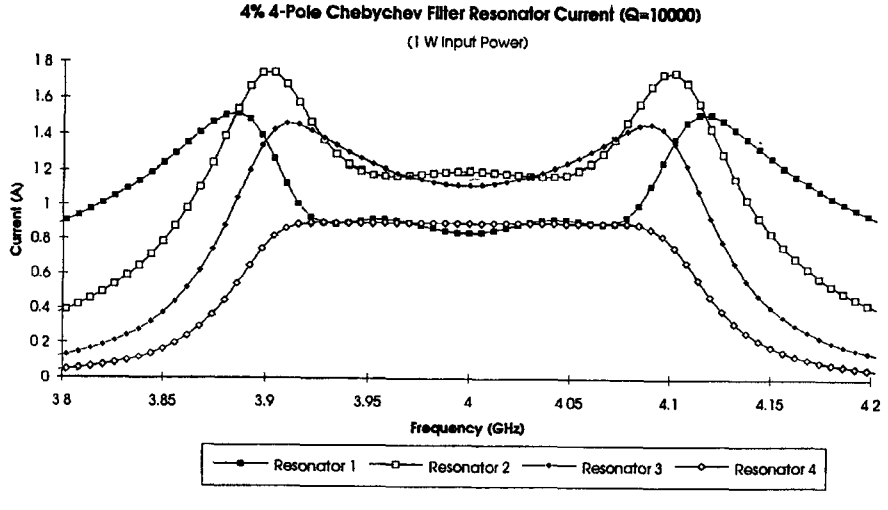

(b)

Fig. 6. The simulated current of two four-pole filters designed with a percentage bandwidth of 1 and 4%.

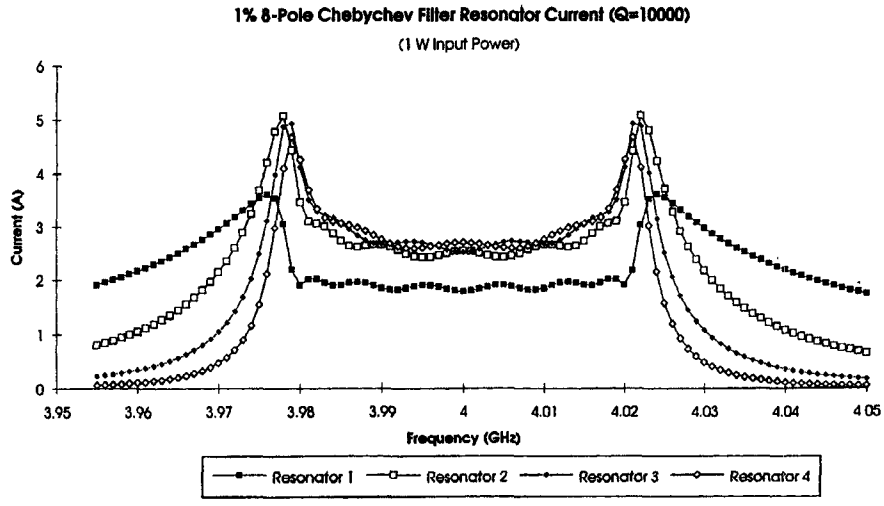

(a)

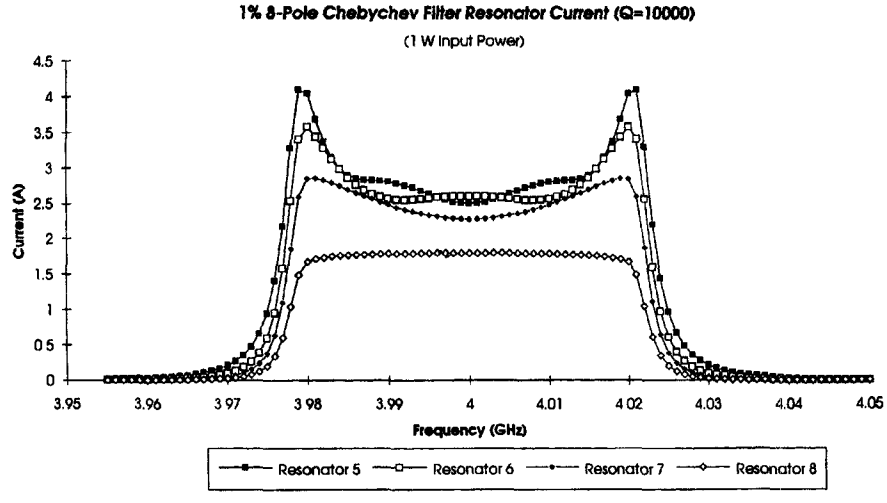

(b)

Fig. 7. The simulated current of an 8-pole filter designed with a 1% percentage bandwidth.

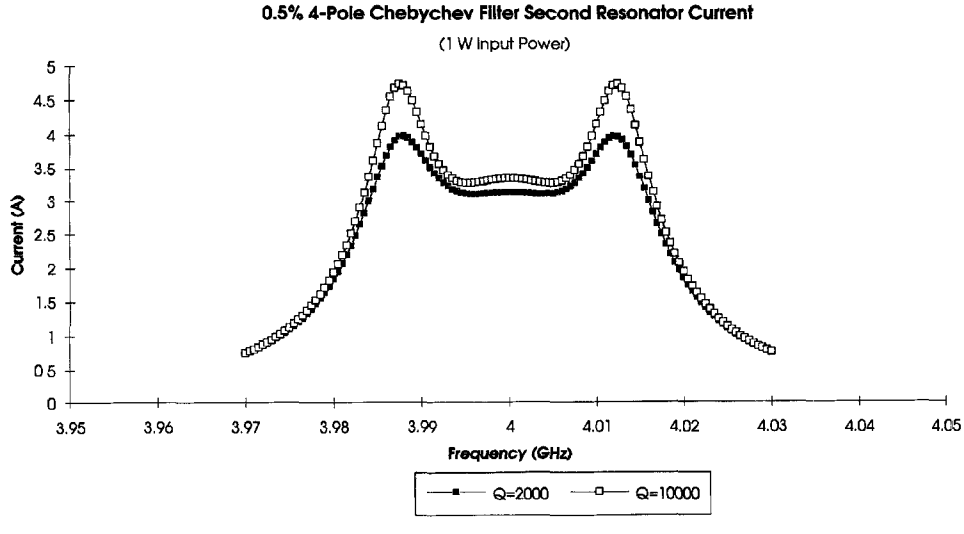

Fig. 8. The current flowing on a four-pole 0.5% bandwidth filter simulated with Q values of 2,000 and 10 000.

TABLE II
HIGHEST RESONATOR CURRENT (A) OF IDEAL CHEBYSHEV FILTERS WITH 1 W INPUT POWER

Poles	Q	Bandwidth						
		0.25%	0.50%	1%	2%	3%	4%	5%
2	5,000	3.593	2.581	1.839	1.306	1.068	0.925	0.828
	10,000	3.650	2.601	1.847	1.309	1.069	0.926	0.829
	20,000	3.679	2.612	1.851	1.310	1.070	0.927	0.829
3	5,000	4.813	3.575	2.600	1.865	1.530	1.329	1.190
	10,000	5.055	3.677	2.638	1.879	1.538	1.333	1.194
	20,000	5.200	3.730	2.657	1.886	1.542	1.336	1.195
4	5,000	5.857	4.520	3.351	2.429	2.000	1.739	1.560
	10,000	6.393	4.739	**3.435**	2.460	2.017	1.750	1.568
	20,000	6.702	4.858	3.479	2.475	2.026	1.756	1.572
5	5,000	6.480	5.151	3.891	2.850	2.356	2.053	1.843
	10,000	7.284	5.503	4.031	2.903	2.385	2.072	1.857
	20,000	7.782	5.701	4.106	2.930	2.400	2.082	1.864
6	5,000	6.844	5.570	4.281	3.169	2.629	2.296	2.063
	10,000	7.877	6.054	4.482	3.247	2.673	2.324	2.084
	20,000	8.561	6.338	4.591	3.287	2.695	2.339	2.095
7	5,000	7.057	5.847	4.560	3.409	2.839	2.484	2.235
	10,000	8.269	6.449	4.821	3.513	2.898	2.523	2.264
	20,000	9.120	6.819	4.968	3.568	2.928	2.543	2.278
8	5,000	7.184	6.029	4.759	3.590	3.012	2.651	2.394
	10,000	8.526	6.731	5.077	3.749	3.112	2.717	2.443
	20,000	9.519	7.180	5.302	3.843	3.164	2.752	2.468
9	5,000	7.261	6.148	4.901	3.785	3.205	2.829	2.560
	10,000	8.695	6.931	5.353	4.001	3.330	2.913	2.621
	20,000	9.802	7.571	5.658	4.119	3.397	2.957	2.653
10	5,000	7.309	6.227	5.005	3.953	3.363	2.976	2.697
	10,000	8.787	7.078	5.590	4.209	3.514	3.078	2.772
	20,000	10.009	7.905	5.952	4.353	3.596	3.132	2.812
11	5,000	7.339	6.279	5.123	4.086	3.492	3.098	2.813
	10,000	8.880	7.245	5.778	4.381	3.668	3.218	2.901
	20,000	10.246	8.171	6.196	4.551	3.765	3.283	2.948
12	5,000	7.359	6.314	5.212	4.191	3.597	3.199	2.908
	10,000	8.930	7.370	5.927	4.523	3.797	3.336	3.010
	20,000	10.423	8.382	6.397	4.718	3.910	3.411	3.068

TABLE III
ESTIMATED POWER HANDLING CAPABILITY OF THE REFERENCE FILTER

HTS filter structures (Examples)	Estimated maximum power of the reference filter
Structure # 1 3-pole, 4 % BW , Q=10,000 P (measured) = 95 watts	P = 14.3 watts
Structure # 2 4-pole, 1 % BW , Q=10,000 P (measured) = 50 watts	P = 50 watts
Structure # 3 8-pole, 1 % BW , Q=10,000 P (measured) = 30 watts	P = 65.5 watts
Structure # 4 5-pole, 3 % BW , Q=20,000 P (measured) = 70 watts	P = 34.2 watts

TABLE IV
THE MAXIMUM POWER OF A THREE-POLE HTS THIN FILM FILTER MEASURED AT THREE DIFFERENT TEMPERATURES

Operating Temperature	Maximum Power
77 K	2 watts
65 K	2.5 watts
20 K	7 watts

TABLE V
THE MAXIMUM POWER LEVEL OF HTS FILTERS MEASURED IN A LIQUID NITROGEN DEWAR AND A MECHANICAL COOLER

Filter	Maximum Power Liquid-Nitrogen Measurement	Maximum Power Mech. Cryo-cooler Measurement
3-pole HTS thin film filter	33.9 dBm	33.3 dBm
4-pole DR/HTS filter	45.7 dBm	45.0 dBm
4-pole DR/HTS filter	47.9 dBm	45.0 dBm

using the same HTS materials and resonator structure. The specifications chosen for the reference filter are:

1) Filter order: four-pole;
2) percentage bandwidth: 1%;
3) unloaded Q: 10 000.

Table II provides the simulated maximum current (assuming an input power of 1 W) for filters designed with different orders, different percentage bandwidth and different unloaded Q values. With the use of Table II, one can easily scale the maximum power level of the measured filter to that of the reference filter. The estimated maximum power level of the reference filter can be written as

$$P_{\text{estimated}} = \left(\frac{I_f}{I_r}\right)^2 \cdot P_{\text{measured}} \tag{2}$$

where, I_r is the simulated maximum current of the reference filter identified in Table II (in bold font) while I_f is the simulated maximum current of the filter that has the same specifications as the measured filter. P_{measured} is the maximum power of the measured filter.

For example, consider structure #1, the test results indicate that the filter is capable of handling 95 W. The estimated maximum power of the reference filter (as if it was built using the same material and resonator structure) would be

$$P_{\text{estimated}} = \left(\frac{1.333}{3.435}\right)^2 \cdot 95 = 14.3\,\text{W}. \tag{3}$$

Similarly, the estimated maximum power of the reference filter for the other three filter structures #2, #3, and #4 can be calculated. A summary of the results achieved is given in Table III. It can be seen that although structure #1 appears to have extremely high power handling capability, in reality, the structure has the worst inherent power handling capability among the four filter structures identified above.

In quoting the power handling capability of HTS filters, it is important to state the definition used for the maximum power level of HTS filters. Qualitatively, the maximum power level is defined as the highest power level before the filter ceases to function as a superconductive filter. The Q of HTS filters typically degrade rapidly as the input power approaches the maximum level. Nevertheless, the criterion used to determine the point where the filter ceases to function should be quantitatively defined. In this paper the maximum power is defined as the power level at which the unloaded Q of the filter degrades by an order of magnitude from the value achievable at an input power of 0 dBm.

It should be pointed out that the reference filter does not have to have the specifications given above. Any other specifications can be chosen. The objective is to have one reference for comparison. The above procedure outlines the main parameters which impact the power handling capability of HTS filters. Other parameters related to high power testing can also have a significant impact on the measured maximum power level an HTS filter may appear to handle. These parameters include:

A. Temperature of Measurements

It is well known that the operating temperature considerably affects the power handling capability of HTS filters. No

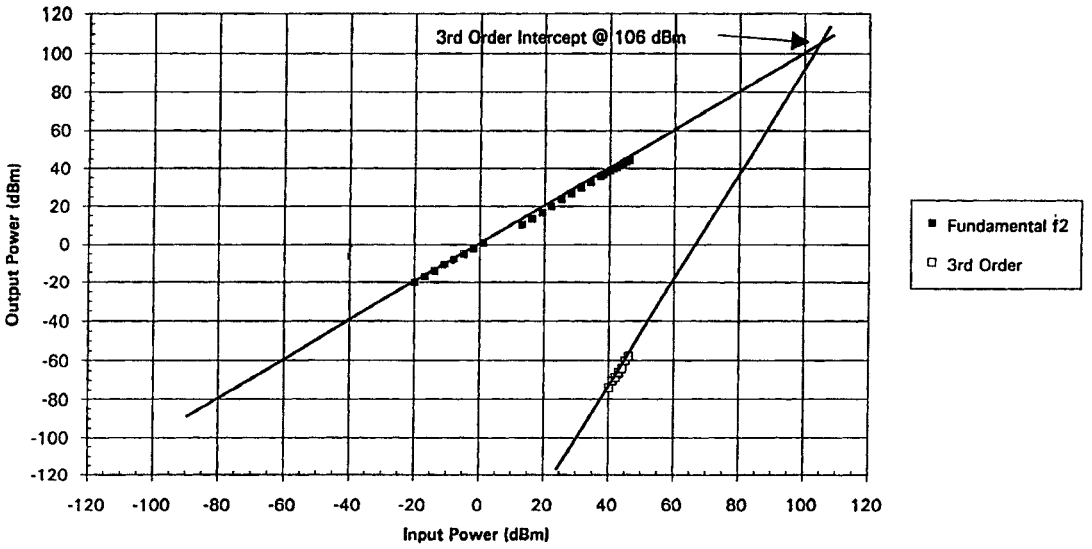

Fig. 9. The passive intermodulation results for the four-pole hybrid DR/HTS filter whose RF performance is given in Fig. 2.

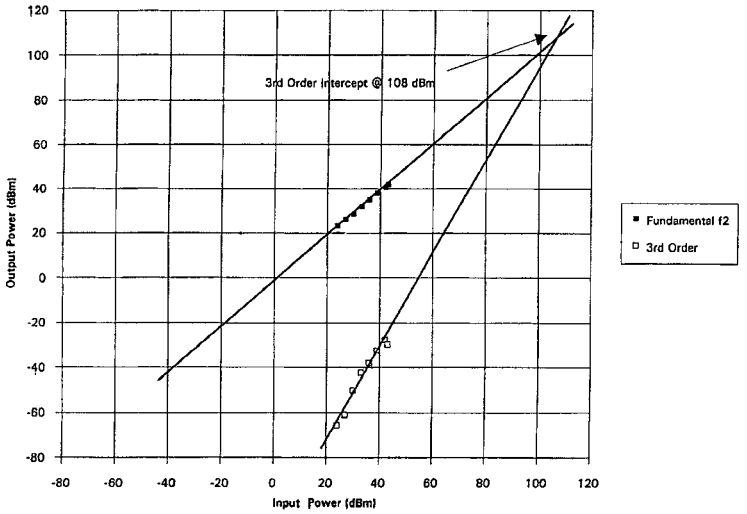

Fig. 10. The passive intermodulation results of an 8-pole hybrid DR/HTS filter.

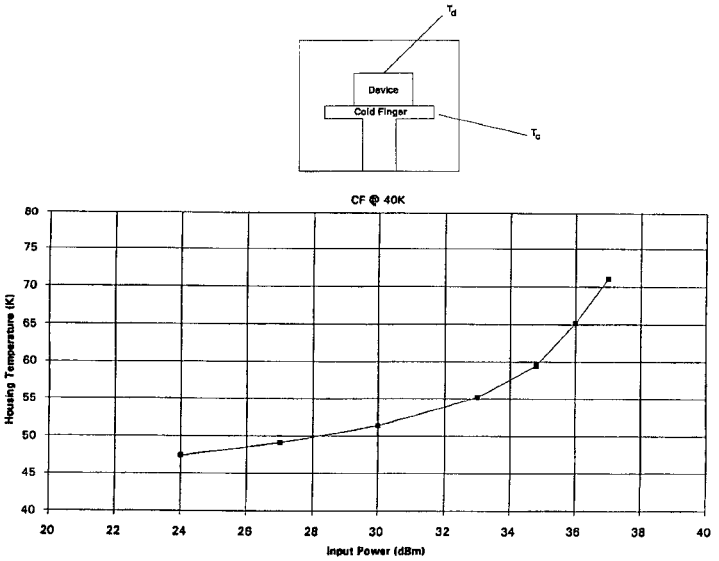

Fig. 11. The temperature of a hybrid DR/HTS filter housing versus input power for a fixed cold finger temperature of 40 K.

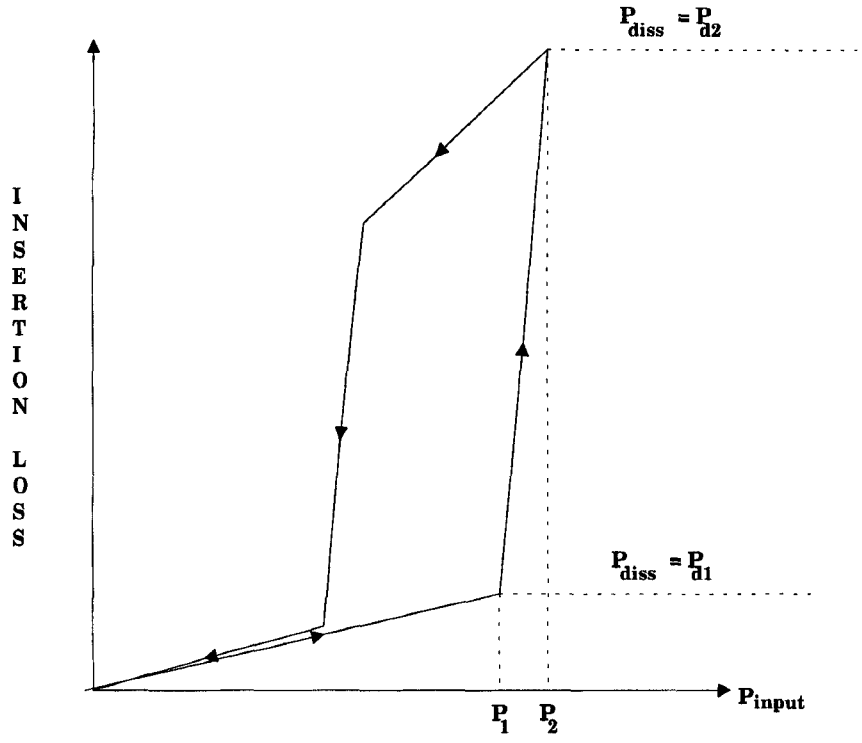

Fig. 12. Insertion loss variation versus input power of HTS filters that handle high power.

theoretical tools are currently available that can accurately predict the power handling capability of HTS filters over temperature. Table IV gives the rated power of a three-pole HTS thin film filter measured at three different temperatures, 77, 65, and 20 K. It can be seen that reducing the operating temperature from 77 to 20 K could increase the power handling capability of this HTS filter by more than three times.

B. Type of Cooling Mechanisms

The type of cooling mechanism (whether it is a liquid nitrogen dewar or a mechanical cryo-cooler) also plays a significant role in determining the maximum power level of HTS filters. The effect of this parameter is more pronounced for HTS filters that handle extremely high power levels. The measured maximum power level handled by the HTS filter may also vary from one cooler to another depending on the cooler design and its cooling capacity.

A number of HTS filters have been tested for high power using liquid nitrogen dewar and a mechanical cryo-cooler of more than 5 W of cooling capacity. A summary of the results achieved is given in Table V. It can be seen that the use of liquid nitrogen dewar typically leads to a higher maximum measured power level than the level which the HTS filter may appear to handle in a mechanical cryo-cooler.

C. Type of Measurements

There are three types of measurements that can be used to evaluate the rated power of HTS filters; CW measurement, sweep measurements, and pulse-modulated measurements. In view of Figs. 6–8 it can be seen that the current generated on the resonators is typically high at the band edge. CW or pulse-modulated testing should therefore be carried out at one of the band-edges frequencies in order to provide a true evaluation of the power handling capability.

The accuracy of measuring high power HTS filters could be also affected by the heat generated from the constant CW signals. Accurate evaluation of the ability of the HTS materials to handle high power requires that the average temperature rise during testing is very small. The use of pulse-modulated signals rather than CW signals helps to minimizing the temperature rise inside the filter. The results presented in Figs. 2–4 are obtained using sweep measurements. The advantages of the sweep measurements over the single-frequency CW measurement is that it allows the observation of performance degradation over the whole band. This type of measurement must be performed in real applications to guarantee that the filter meets all specified requirements while operating at high power.

V. Passive Intermodulation Testing

Passive intermodulation products (PIM) have been known to be a potential problem in high power filters. In conventional waveguide and dielectric filters, PIM arises primarily due to the formation of very thin oxide layers on metal surfaces, mechanical imperfections on the joints or both. Nonlinearity in such components could also arise due to micro-cracks and voids in metal structures or due to metal particles.

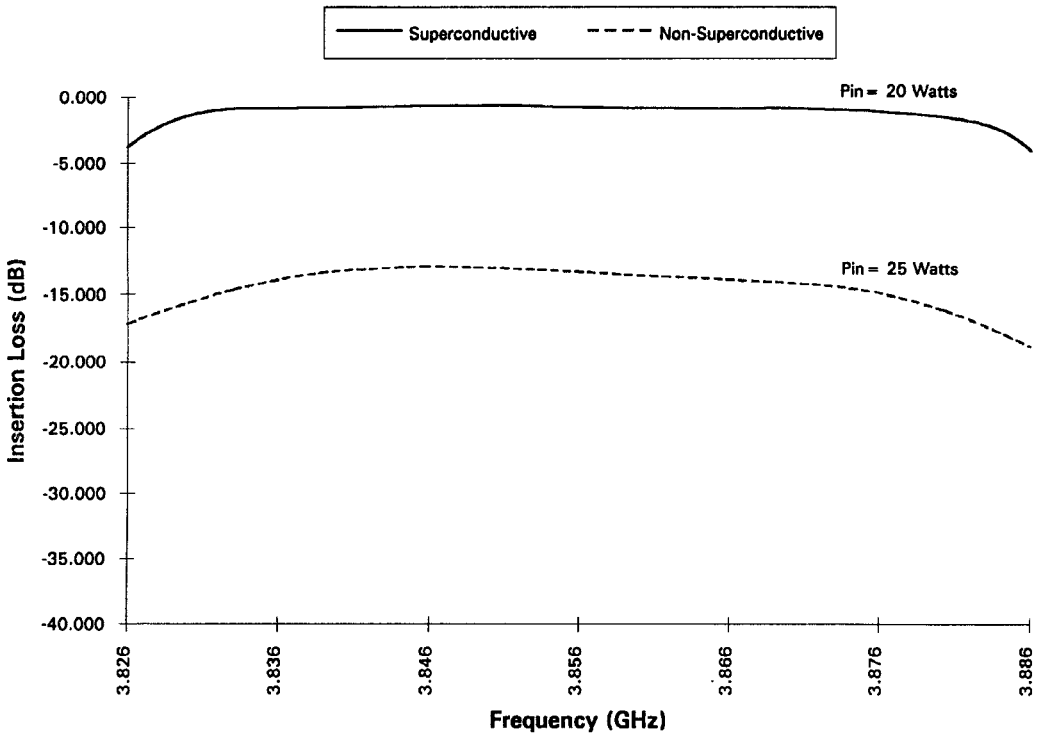

(a)

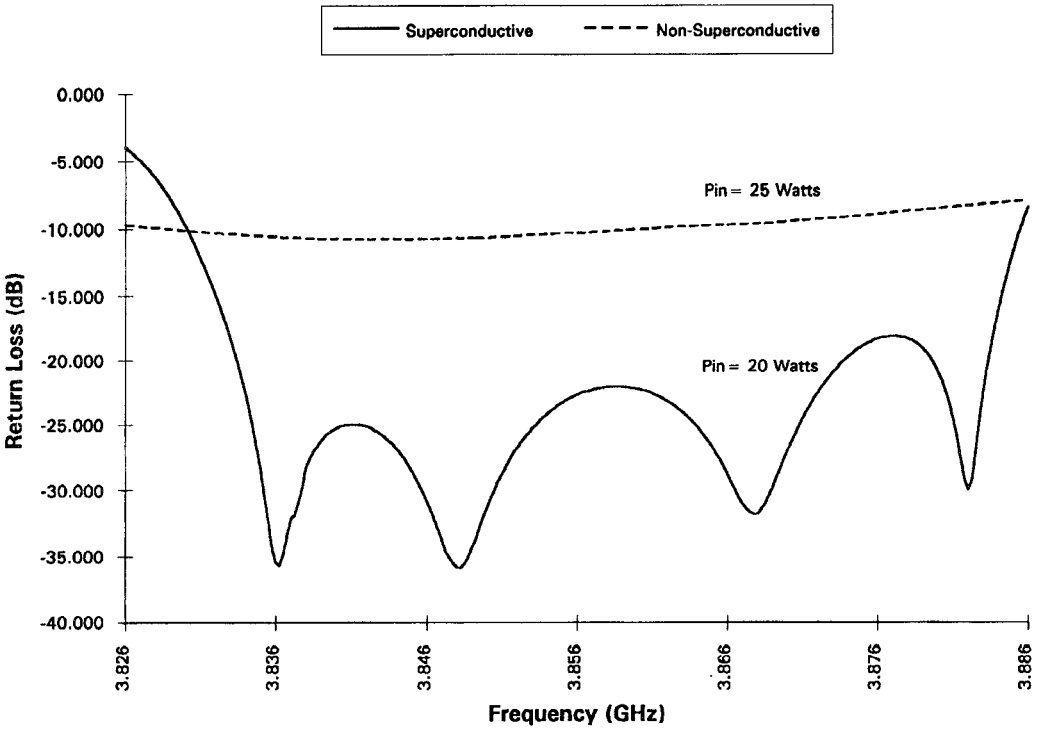

(b)

Fig. 13. The measured insertion loss and return loss results of a four-pole HTS filter as it switches from the superconductive state to the non-superconductive state.

In HTS components the main source of nonlinearity is the HTS material itself—the surface resistance of HTS films is not only a function of temperature and frequency but also a function of local RF fields. This in turn can result in harmonic generation at relatively low power levels [2] and [5].

Fig. 9 illustrates the passive intermodulation results for the four-pole HTS filter whose RF performance is given in Fig. 2.

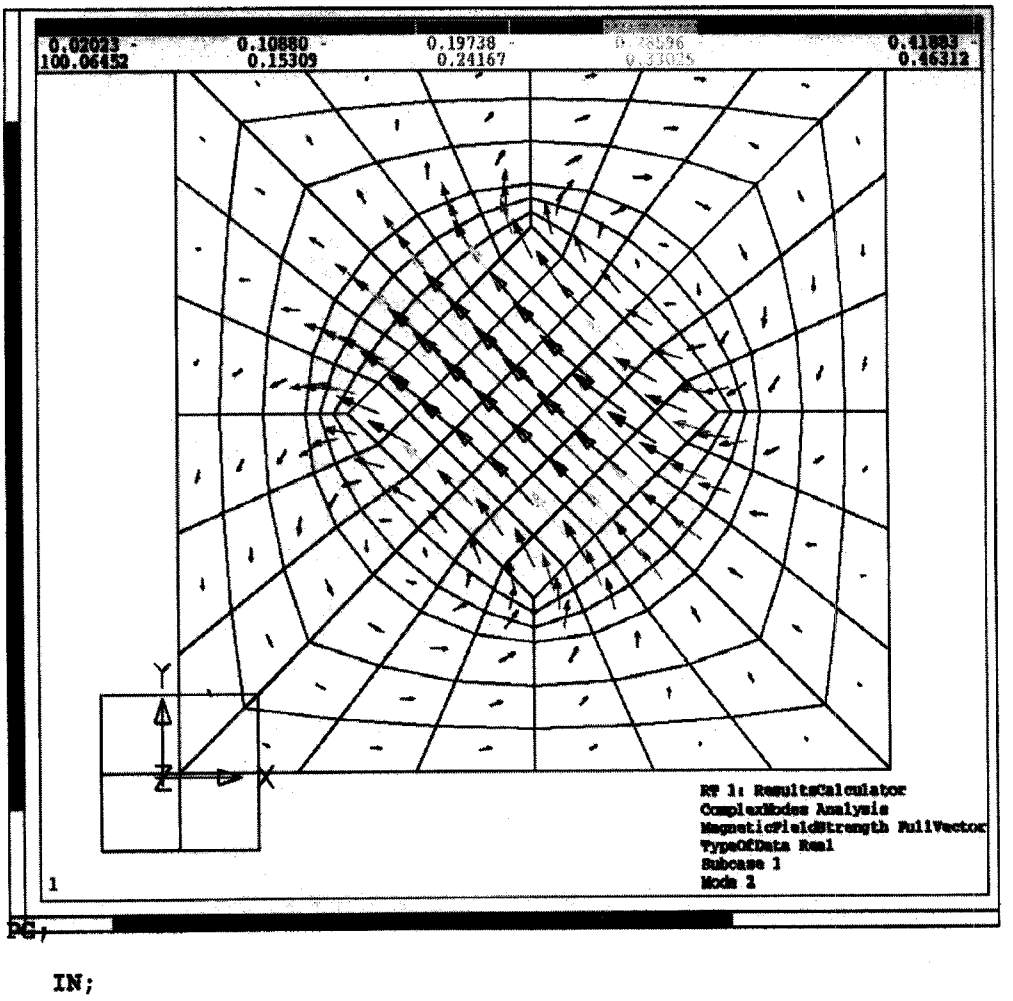

Fig. 14. The magnetic field distribution inside a hybrid DR/HTS resonator operating in a dual-mode (only one mode is shown in this figure).

The filter has a third-order intercept point of 106 dBm. The results achieved for the 8-pole version of this filter are given in Fig. 10.

VI. Thermal Analysis of High Power HTS Filters

For HTS filters that handle high power levels, the heat generated inside the filter may be high enough to drive the HTS material out of the superconductive state. Fig. 11 illustrates the temperature of a hybrid DR/HTS filter housing versus input power for a fixed cold finger temperature of 40 K. At low power the temperature of the filter housing is only few degrees higher than that of the cold finger. As the input power increases, a significant rise in the filter housing temperature over that of the cold finger is observed indicating that there is a considerable amount of heat generated inside the filter structure.

The typical insertion loss-versus input power of HTS filters that handle high power levels is shown in Fig. 12. The insertion loss increases gradually as the input power increases. At an input power P_1 the filter is still in the superconductive state and the power dissipated in the filter is P_{d1}. As the input power increases slightly to P_2 the HTS filter loses its superconductive characteristics, leading to a considerable increase in the insertion loss which in turn leads to larger increase in power dissipation P_{d2}.

To demonstrate the amount of heat dissipated inside the filter structure, Fig. 13 illustrates the measured insertion loss and return loss results of a four-pole HTS filter as it switches from the superconductive-state to the nonsuperconductive state. it can be readily shown that the power dissipated in the filter is given by:

1) Superconductive state: $P_1 = 20$ W, insertion loss = 0.64 dB, and return loss = 20 dB. Power dissipated $(P_{d1}) = 2.7$ W;
2) nonsuperconductive state: $P_2 = 25$ W, insertion loss = 13.88 dB, and return loss = 9.7 dB. Power dissipated $(P_{d2}) = 21.4$ W.

Once the filter switches to the nonsuperconductive state, reducing the input power to P_1 does not necessarily get the filter back to its superconductive state. The heat generated in the nonsuperconductive state may be large enough to exceed the available cooling power, which in turn prevents the filter from returning to the superconductive state even when the

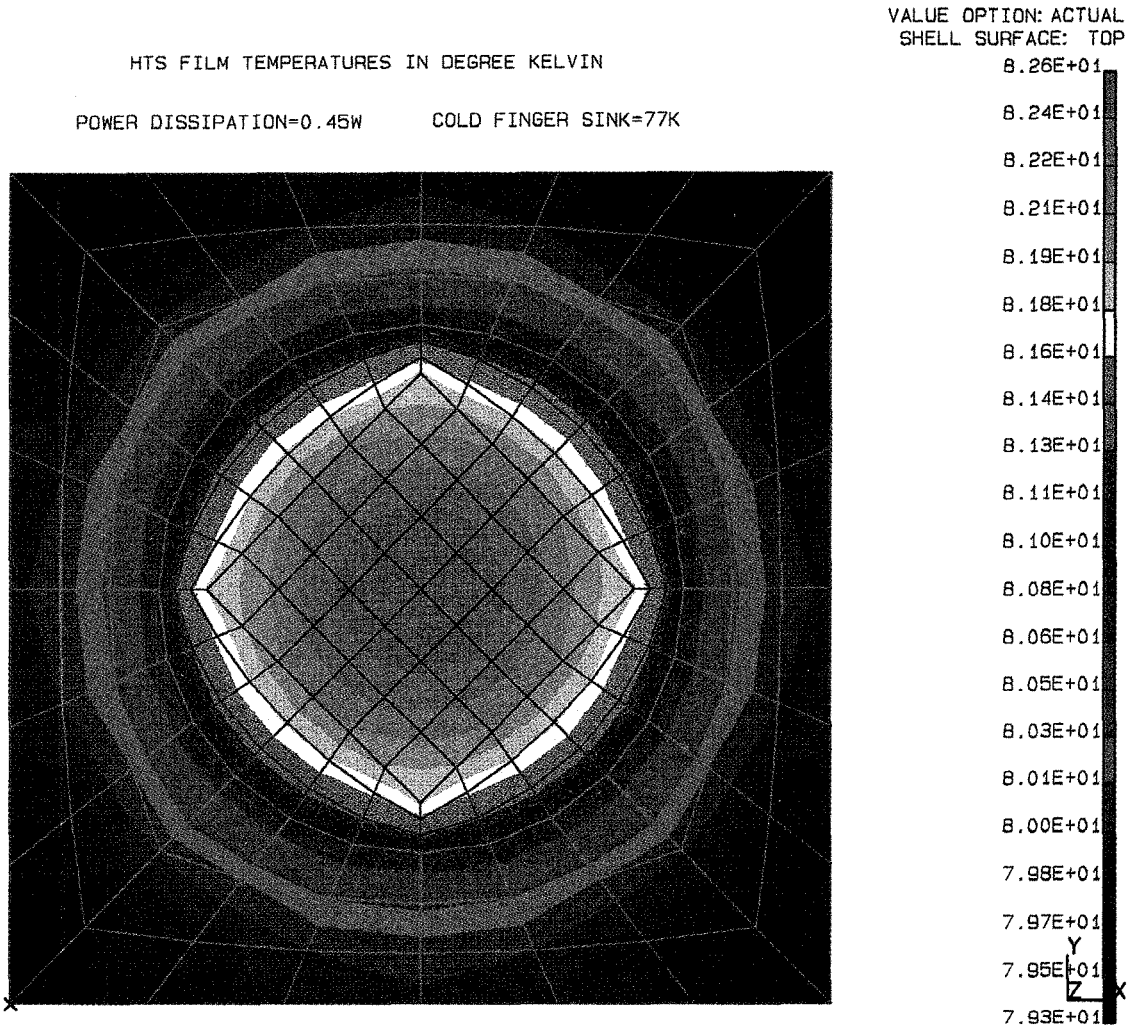

(a)

Fig. 15. The temperature variation inside a hybrid DR/HTS resonator assuming a power dissipation of 0.45 W.

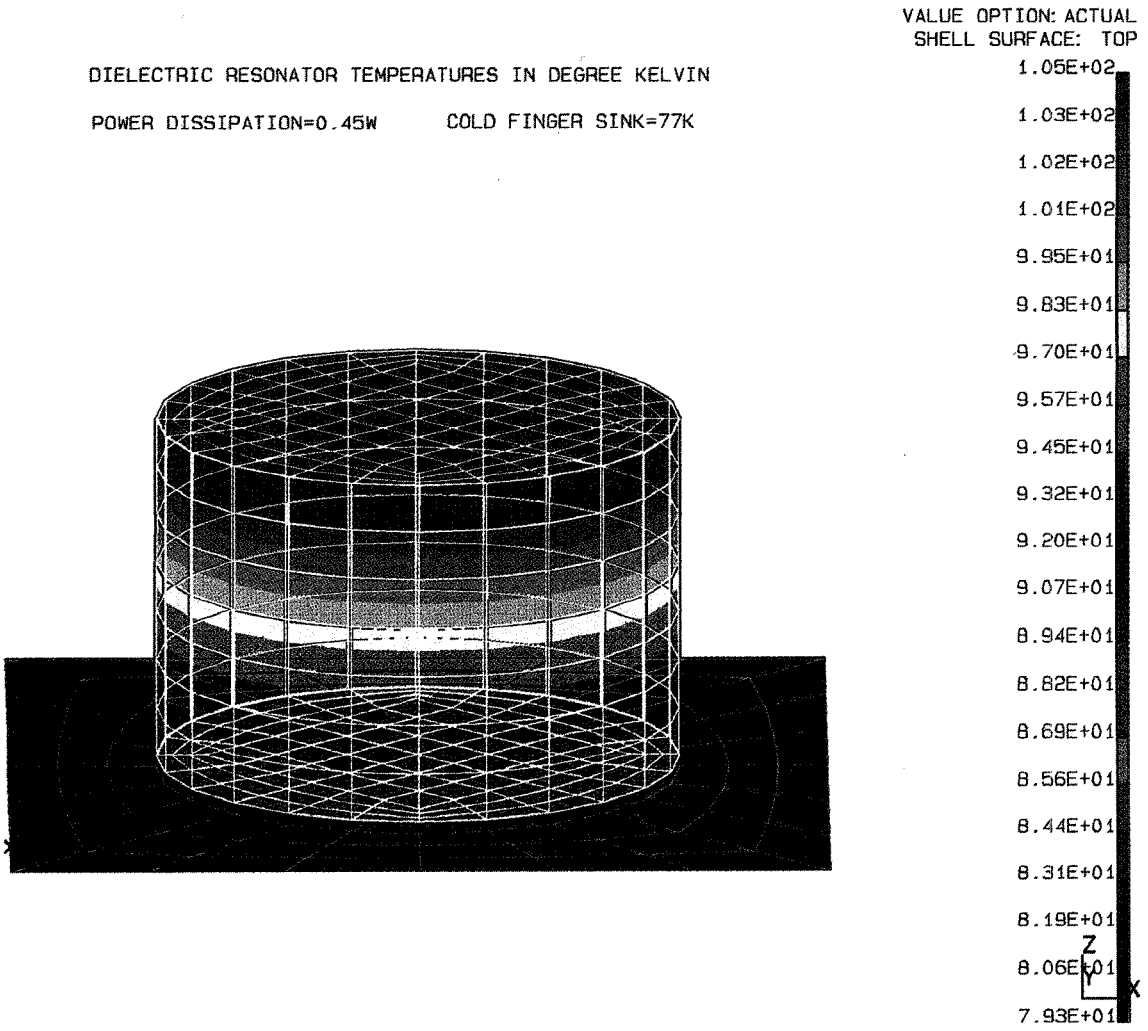

(b)

Fig. 15. *(Continued.)* The temperature variation inside a hybrid DR/HTS resonator assuming a power dissipation of 0.45 W.

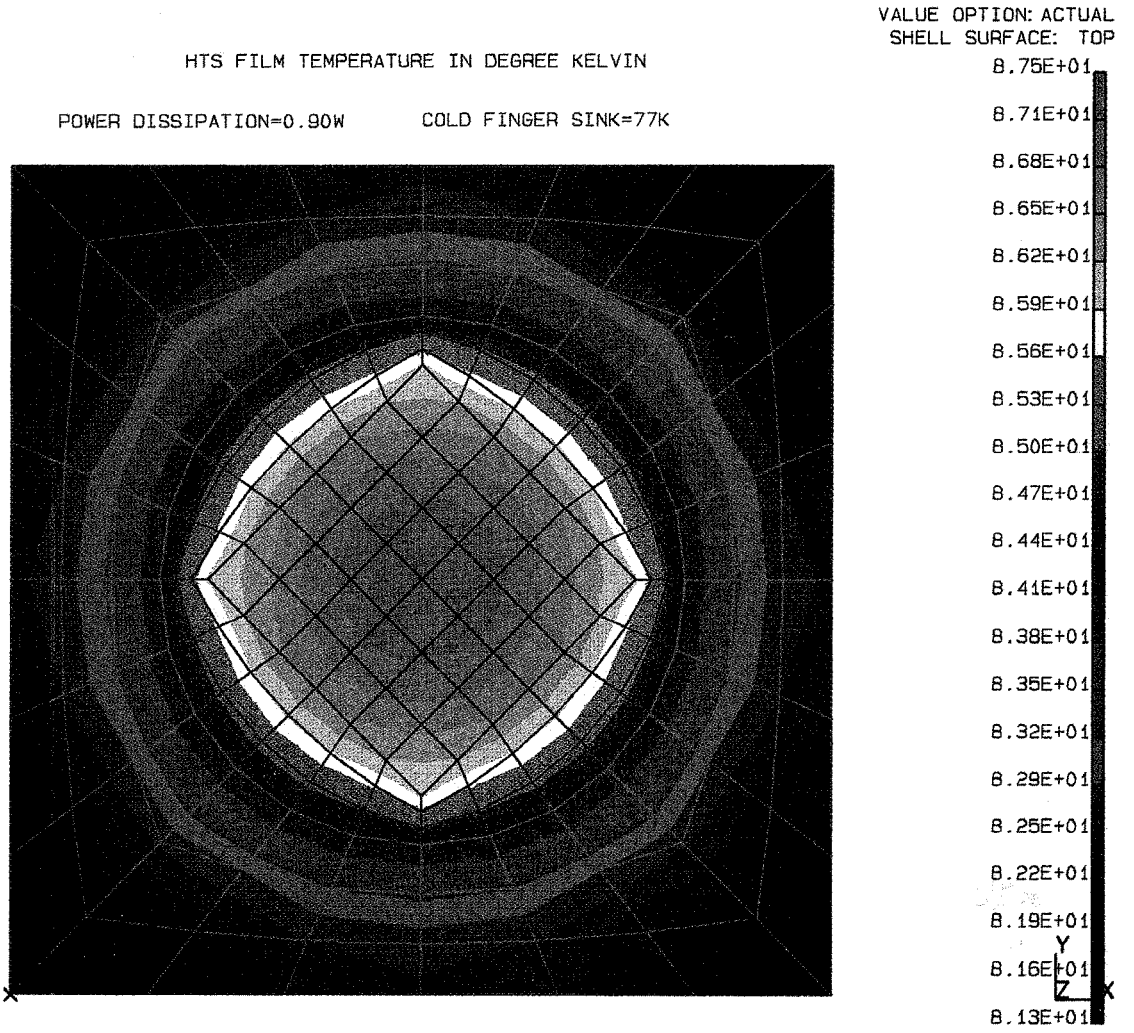

(a)

Fig. 16. The temperature variation inside a hybrid DR/HTS resonator assuming a power dissipation of 0.9 W.

input power is below P_1. In general, the input power has to be considerably reduced to get rid of the heat before the filter switches back to the superconductivity state. The filter insertion loss versus input power follows then the hysteresis-type curve shown in Fig. 12.

The above discussion demonstrates the importance of performing thermal analysis of HTS filters. Generally, the heat generated inside HTS filters is not uniformly distributed. The heat may be concentrated in an area close to the HTS films which in turn can cause a considerable temperature rise in this area. Such temperature rise will degrade the surface resistance of the HTS materials and will reduce the current carrying capability of HTS materials. This problem is more pronounced in HTS filters that are capable of handling extremely high power levels such as hybrid DR/HTS filters.

The temperature rise inside hybrid DR/HTS filters is mainly impacted by the mode type, loss tangent of the substrate, and thermal conductivity of the different materials used to construct the resonator. The power handling capability of the HTS filters can thus be improved by optimizing these parameters to minimize the temperature rise in areas close to the HTS films. A finite element software package is used to simulate electromagnetic field distribution and power loss densities within hybrid dielectric HTS resonators operating in different modes. The power loss densities output from the software package are then used as heat generating inputs to determine the temperature variation inside the resonator.

Fig. 14 illustrates the electromagnetic field distribution inside a hybrid DR/HTS resonator operating in a dual HE mode (only one mode is shown in this figure). The temperature variation along the HTS film and the DR resonator, assuming a power dissipation of 0.45, is given in Fig. 15. With the temperature of the cold finger maintained at 77 K, the temperature along the HTS film can vary from 79.3–82.5 K, while the temperature of the resonator itself can be as high as 105 K. Fig. 16 shows the results obtained assuming that the power dissipation is 0.9 W. In this case, the temperature of the HTS film varies from 81.3–87.5 K, while that of the DR resonator varies from 81.3–131 K. It is observed that the theoretical results shown in Figs. 15 and 16 are in good correlation with the measured data given in Fig. 11. With the

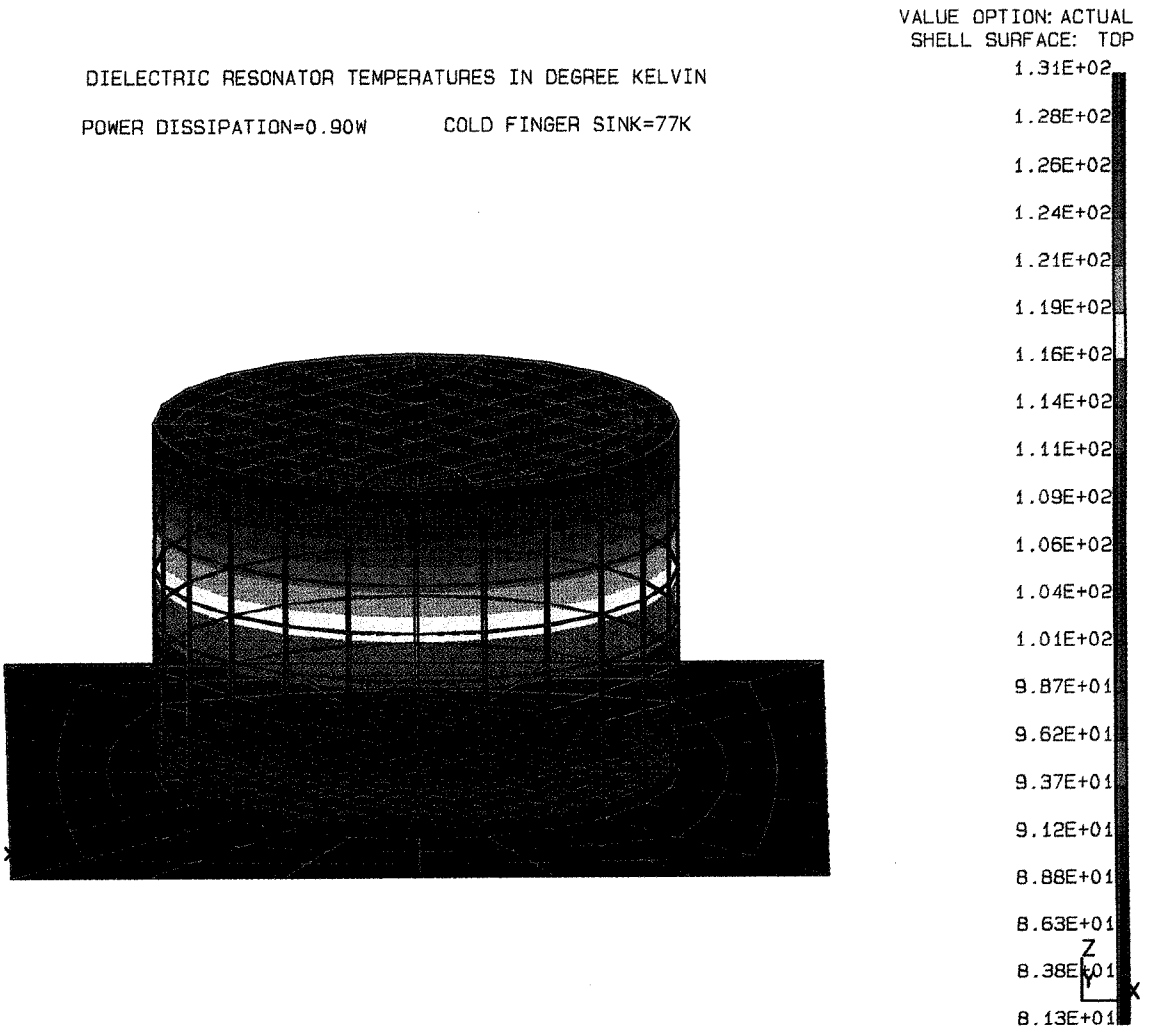

(b)

Fig. 16. *(Continued.)* The temperature variation inside a hybrid DR/HTS resonator assuming a power dissipation of 0.9 W.

optimum choice of the thermal conductivity of the different materials used to construct the hybrid DR/HTS resonator the temperature rise where the HTS films are located can be minimized.

It is important however to mention that due to the fact that the thermal performance of HTS filters is also controlled by the outside cooling environment, these CAD tools are not expected to provide the exact temperature values inside the HTS filter. They are useful in optimizing the filter thermal design by providing qualitative information concerning the temperature distribution inside the HTS filter.

VII. Conclusion

A procedure has been presented for comparing the power handling capability of different HTS filter structures. The maximum power level that an HTS filter seems to handle does not necessarily reflect the true power handling capability of the filter structure. One should take into account the filter order, filter bandwidth, achievable Q and operating temperature when assessing the power handling capability of different HTS filter structures. The type of cooling mechanism, used during testing, may also considerably affect the measured maximum power level. The use of a liquid nitrogen dewar may result in measured maximum power levels that are 0.5–2 dB higher than those obtained using a mechanical cryo-cooler.

It has been observed that the insertion loss versus input power of high power HTS filters follows a hysteresis-type curve. In actual operating systems, such dependence may have a strong impact on the cooling requirements and/or the operating power level of high power HTS filters.

The results presented in this paper demonstrate that the power handling capability of hybrid DR/HTS filters far exceeds that of HTS thin film filters. The ability of an HTS filter to handle high power levels is not only governed by the filter geometry but also by the quality of the HTS materials. The high power levels reported in this paper clearly demonstrate the significant improvement in the quality of today's HTS films, and confirm the

feasibility of designing HTS filters for microwave high power applications.

REFERENCES

[1] R. B. Hammond *et al.*, "Superconducting TIBaCaCuO thin film microstrip resonator and its power handling performance at 77 K," *IEEE Microwave Theory Tech.-S Symp. Dig.*, 1990, pp. 867–870.

[2] A. Fathy, K. Kalokitis, and E. Belohoubek, "Critical design issues in implementing a YBCO superconductor X-band narrow bandpass filter operating at 77 K," *in IEEE Microwave Theory Tech.-S Symp. Dig.*, 1991, pp. 1329–1332.

[3] W. L. Holstein, "Power handling capability of large area HTS thin films at microwave frequencies," in *5th Int. Symp. Superconductivity,* Nov. 1992.

[4] D. E Oates, A. C. Anderson, D. M. Sheen, and S. M. Ali, "Stripline resonator measurements of Zs versus H_f in thin films," *IEEE Trans. Microwave Theory Tech.*, vol. 39, pp. 1522–1529, Sept. 1991.

[5] P. P. Nguyen, D. E. Oates, G. Dresselhaus, and M. S. Dresselhaus, "Nonlinear surface impedance for YBCO thin film: Measurements and a coupled-grain model," *Phys. Rev. B,* vol. 48, pp. 6400–6412, Sept. 1993.

[6] Z. Y. Shen, *High Temperature Superconducting Microwave Circuits.* London: Artech House, 1994.

[7] Z. Y. Shen and C. Wilker, "Raising the power handling capacity of HTS circuits," *Microwaves & RF J.*, Apr. 1994.

[8] G. C. Liang *et al.*, "High power HTS microstrip filters for wireless communications," *IEEE Trans. Microwave Theory Tech.*, vol. 43, pp. 3021–3027, Dec. 1995.

[9] Workshop notes, "High power superconducting microwave technology," in *IEEE Microwave Theory and Tech.-S Symp. Workshop,* May 1994.

[10] G. L. Mattaei and G. L. Hey-Shipton, "Concerning the use of high temperature superconductivity in planar microwave filters," *IEEE Trans. Microwave Theory Tech.*, vol. 42, pp. 1287–1293, July 1994.

[11] Workshop notes, "System applications of high power temperature superconductors and cryogenic electronics," in *IEEE Microwave Theory and Tech.-S Symp. Workshop,* May 1995.

[12] R. R. Mansour *et al.*, "A C-band superconductive input multiplexer for communication satellites," *IEEE Trans. Microwave Theory Tech.*, vol. 42, pp. 2472–2479, Dec. 1994.

[13] R. R. Mansour, "Design of superconductive multiplexers using single-mode and dual-mode filters," *IEEE Trans. Microwave Theory Tech.*, vol. 42, pp. 1411–1418, July 1994.

[14] R. R. Mansour *et al.*, "Design considerations of superconductive input multiplexers for satellite applications," *IEEE Trans. Microwave Theory Tech.*, vol. 44, no. 7, p. 1213–1228.

[15] R. J. Cameron, "General prototype network synthesis methods for microwave filters," *ESA J.*, vol. 6, 1992.

[16] G. L. Matthaei, L. Young, and E. M. T. Jones, *Microwave Filters, Impedance Matching Networks and Coupling Structures.* New York: McGraw-Hill, 1964.

Raafat R. Mansour (S'84–M'86–SM'90) , for a photograph and a biography, see this issue, p. 1227.

Bill Jolley, for a photograph and a biography, see this issue, p. 1228.

Shen Ye (S'88–M'92), for a photograph and a biography, see this issue, p. 1227.

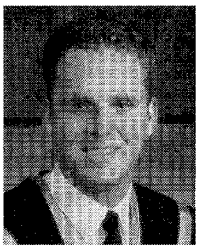

Fraser S. Thomson (S'91–M'92) received the B.Sc.E. degree in electrical engineering with honors from Queen's University, Kingston, Ontario, in 1992. Since January of 1993, Fraser has been studying for the M.Eng. degree in electrical engineering at McMaster University, Hamilton, Ontario.

In May 1992, he joined the Remote Sensing Group of COM DEV Ltd., Cambridge, Ontario, where he was an Engineer on the NASA Scatterometer (NSCAT) program. In June 1993, he joined COM DEV's Corporate Research and Development Department where he has been involved with the design of microwave components using HTS thin films.

Van Dokas, for a photograph and biography, see this issue, p. 1228.